INVITED FEATURE PAPER

Nanoindentation of high-purity vapor deposited lithium films: A mechanistic rationalization of the transition from diffusion to dislocation-mediated flow

Erik G. Herbert,[a] Stephen A. Hackney, and Violet Thole
Department of Materials Science and Engineering, Michigan Technological University, Houghton, Michigan 49931, USA

Nancy J. Dudney
Materials Science and Technology Division, Oak Ridge National Laboratory, Oak Ridge, Tennessee 37830, USA

P. Sudharshan Phani
International Advanced Research Centre for Powder Metallurgy and New Materials, Hyderabad, Telangana–500005, India

(Received 23 December 2017; accepted 29 March 2018)

Nanoindentation experiments performed in high-purity vapor deposited lithium films at 31 °C reveal a strain rate and length scale dependence in the stress at which pop-in type events signal an abrupt transition from diffusion to dislocation-mediated flow. The stress level at which the transition to dislocation-mediated flow occurs varies with the strain rate and ranges from 88 to 208 times larger than the nominal yield strength of bulk, polycrystalline lithium. Variation in the indentation strain rate reveals the relationship between the stress required to initiate the transition and the length scale at which the transition occurs follows the power-law relation, hardness × depth$^{1.17}$ = 1.545 N/m$^{0.83}$, where the magnitude of the exponent and constant reflect the defect structure of the film. A rationalization of the transition is provided through direct comparisons between the measured cumulative distribution function (CDF) and the CDF hypothesized for the activation of a Frank–Read source.

I. INTRODUCTION

Motivated by the need to better understand small-scale mechanical behavior at the lithium/solid electrolyte (Li/SE) interface, nanoindentation experiments have been performed in high-purity 5 and 18 μm thick vapor deposited polycrystalline Li films at 31 °C (homologous temperature, T_H, of 0.67) to ascertain how the hardness of Li changes as a function of length scale and strain rate. Such a study is of particular relevance given the micro-compression experiments recently performed by Xu et al.[1] on single crystal lithium pillars (height to diameter ratios between 3:1 and 5:1) at 26 °C. Their results show that under a constant nominal strain rate of 5 × 10^{-3} s^{-1}, the compressive yield strength increases from 15 to 105 MPa as the pillar diameter decreases from 9.45 to 1.39 μm. The size-dependent yield strength ranges from 30 to 210 times larger than the reported yield strength (~0.5 MPa) of bulk polycrystalline Li near room temperature.[1,2]

Despite the potential for experimental artifacts such as, but not limited to, surface radiation damage and contamination effects in the pillar experiments, we report that Xu's results are generally consistent with our own experimental observations using nanoindentation.[3] In the results presented here, the relationship between the indentation depth and the transition from diffusion to dislocation-mediated flow (taken to be the mean pressure or hardness at the first dislocation avalanche) is revealed through a variation in the indentation strain rate. As in the pillar study, the indentation results reported here show an inverse relationship between length scale and stress at the initiation of dislocation-mediated flow. In light of the similar results obtained by the two uniquely different yet complimentary measurement techniques, we note that a significant fraction of the surface layer radiation damage caused by FIB milling of the pillars may have been fortuitously eliminated by annealing, as the room temperature sample preparation and experiments were performed at T_H = 0.66. The similar results further suggest that the effect of solid solution strengthening from the implanted Ga^+ in the pillars is minor.

The increase in strength of Li at small length scales observed in the pillar compression and nanoindentation experiments has significant implications for the design of next generation energy storage devices that may employ

[a]Address all correspondence to this author.
e-mail: eherbert@mtu.edu
Corresponding Editor: Erik Herbert
This paper has been selected as an Invited Feature Paper.
DOI: 10.1557/jmr.2018.85

solid state, ceramic electrolytes. High modulus, low toughness solid electrolytes (SEs) can be sensitive to stress intensification resulting from electrochemical deposition and growth of Li into small-scale defects and pores at the Li/SE interface, potentially causing mode I fracture and enabling the subsequent growth of Li dendrites into the breach.

As explained by Xu et al.,[1] one potential explanation for the size-dependent strength in the Li pillar compression experiments is a low initial dislocation density and, hence, dislocation nucleation governed plasticity. Similar arguments have been put forth for the rationalization of high hardness pop-in events that signal the onset of dislocation-mediated flow during nanoindentation.[4] More recently, many investigators have examined the possibility that the enhanced strength uniquely observed at small length scales in pillars, thin films, wires, and even small grain size is controlled by dislocation source activation rather than ex nihilo dislocation nucleation.[4–8] In addition to confirming the high strength associated with dislocation motion, we show for the first time how a hypothesized cumulative distribution function (CDF) for the activation of a Frank–Read source can be used to rationalize the elevated stress at the transition to dislocation-mediated flow. Collectively, the results and analysis reported here provide the first mechanistic rationalization of the unexpectedly high strength of Li at the length scale of defects at the Li/SE interface.

II. EXPERIMENTAL METHODS

Details of the Li film deposition and the nanoindentation system have been previously reported.[9] To avoid unnecessary duplication, the unique aspects of determining the hardness as a continuous function of indentation depth and strain rate are not revisited here, but are readily available in a previous publication.[3]

III. RESULTS AND DISCUSSION

Verification of the measurement system's load and displacement calibrations, the frame stiffness, and the indenter tip's area function have been previously reported.[9] Similarly, the load–displacement behavior and the depth and strain rate dependent hardness of high-purity polycrystalline 5 and 18 μm thick Li films on glass substrates (T = 31 °C) have been reported as well.[3] Collectively, these experimental observations lead us to hypothesize that the previously reported strain bursts signify an abrupt transition from diffusion to dislocation-mediated flow that is triggered by the combination of a critical threshold in stress and length scale, as the dislocation mechanism appears to require not only the necessary driving force, but also sufficient room to physically operate. Here we examine this conjecture by attempting to show how a hypothesized CDF for the activation of a Frank–Read source can be used to rationalize the elevated stress at the transition to dislocation-mediated flow.

A. Rationalization of a sudden transition to dislocation-mediated flow

Figure 1 shows the hardness, H, as a continuous function of indentation depth, h, measured at a targeted $\dot{P}/P$ of 0.05 s^{-1}. The triangular data points represent the average of 56 measurements and the scatter bars span one standard deviation about the mean. The individual curves (small circular data points) represent 6 of the 56 measurements used to calculate the average H. Illustrated by the individual curves, the sudden transition from diffusion to dislocation-mediated flow occurs with an abrupt avalanche of dislocation motion and a simultaneous drop in the mean pressure. We note this observation is very similar to the indentation behavior of indium (tetragonal, rather than the body centered cubic crystal structure and T_H = 0.69 at room temperature) previously reported by Feng and Ngan.[10] Here, the stress and depth at which the transition occurs as well as the magnitude of the ensuing pressure drop clearly varies from one test site to the next, presumably in a manner that directly reflects the details of the defect structure in the volume of the material being sampled by the indenter. The inflection point in the average H corresponds to the average depth at which the sudden transition from diffusion to dislocation-mediated flow occurs. As previously reported,[3] the average H as a function of depth and position across the surface of the specimen is quite repeatable despite the large scatter shown in Fig. 1. On average and in a manner that

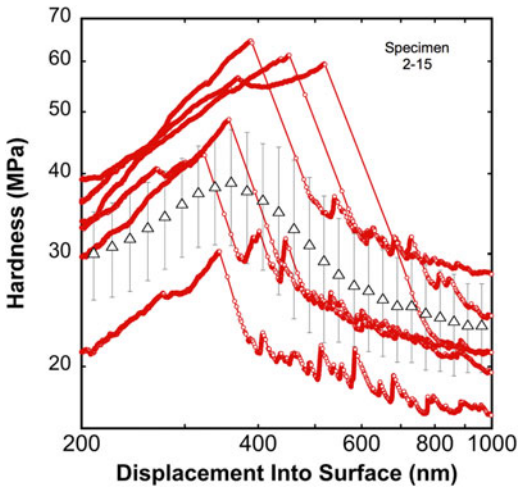

FIG. 1. The hardness of a 5 μm thick high-purity vapor deposited Li film on a glass substrate. Measured at T_H = 0.67 and a targeted $\dot{P}/P$ of 0.05 s^{-1}. Averaged results (triangular data points) and 6 of 56 individual curves that illustrate the abrupt transition from diffusion to dislocation-mediated flow.

depends on the indentation strain rate, the mean contact pressure required to initiate the dislocation-mediated flow at a T_H of 0.67 is found to range from approximately 44 to 104 MPa (this range decreases slightly, from 40 to 90 MPa, when the displacement burst filter described in Sec. III.B. is not considered).

The plastic deformation before the strain burst (pop-in) has been rationalized using diffusional creep mechanisms.[3] A natural outcome of that rationalization is that prior to the strain burst, there is little to no change in the dislocation density. As such, there is no elastically constrained volume of plastically deformed Li beneath the indenter and, therefore, the constraint factor relating H to the flow stress of Li is taken to be 1. Assuming the yield strength of bulk polycrystalline Li is 0.5 MPa near room temperature, a constraint factor of 1 means the mean pressure required to initiate dislocation-mediated plasticity ranges from approximately 88 to 208 times higher than the yield stress of bulk polycrystalline Li.

These high pressures are generally consistent with the results from microcompression experiments recently performed by Xu et al.[1] on single crystal Li pillars (height to diameter ratios between 3:1 & 5:1) at a T_H of 0.66 (T = 26 °C). Examined under a constant nominal strain rate of 5×10^{-3} s^{-1}, their results show the compressive yield strength increases from 15 to 105 MPa as the pillar diameter decreases from 9.45 to 1.39 μm (approximately 30–210 times larger than the yield stress of bulk polycrystalline Li). Similar to the nanoindentation results, the onset of dislocation-mediated flow in the pillars is concomitant with an apparent avalanche of dislocation motion. Post-test images clearly show slip-offsets in the pillars that are oriented at or near 45° to the applied load. As explained by Xu, the size-dependent strength of the pillars may be the direct result of a low initial dislocation density and, hence, dislocation nucleation governed plasticity. We also note that due to the high T_H and the potentially low dislocation density, creep mechanisms such as Nabarro–Herring and Harper–Dorn could contribute to the deformation of the pillar prior to the onset of dislocation-mediated flow.

The results from the indentation experiments represent five data sets comprising a total of 268 measurements performed at three targeted values of $\dot{P}/P$, 0.05, 0.5, and 1.0 s^{-1}, and a constant loading rate of 12.5 μN/s. Figure 2 shows the average avalanche stress (H) and the corresponding average avalanche depth at the onset of dislocation-mediated flow for two films and five strain rates. As previously reported, due to the nature of the loading algorithms and the depth-dependent H, the indentation strain rates are unavoidably depth dependent.[3] The values of $\dot{h}/h$ immediately prior to the avalanche are reported in Fig. 2. As the data show, there is a significant size effect in that the transition or avalanche stress varies with depth, with a power-law exponent of −1.17. This value is nearly double that observed in the microcompression experiments performed by Xu et al.[1] (−0.68 at a slightly lower T_H), but rather than being related to the physical dimensions of the test specimen, the size effect observed here is controlled by the size of the indentation stress field in relation to the defect structure being sampled by the indenter.[4] Following the logic proposed by Bragg[11] in 1942, argued by El-Awady[7] in 2015, and demonstrated by Li et al.[8] in 2016, the power law exponent of −1.17 is generally consistent with the Orowan mechanism. That is to say the stress level required to activate the weakest dislocation source is inversely proportional to the source length and its inherent curvature, both of which are in turn bounded by the physical dimensions of the stress field responsible for activating the source.[8]

As proposed by Stricker and Weygand[6] in 2015 and in general agreement with the literature review of "Plasticity in Confined Dimensions," by Kraft et al.[5] in 2010, we note the dislocation avalanche and simultaneous pressure drop is consistent with dislocation multiplication enabled by a glissile junction that effectively operates as a Frank–Read source. The strength-controlling dimension would thus be the distance between the pinning points of the junction, as this length determines the curvature of the dislocation and, therefore, the stress level required to activate it. As shown in Fig. 3, the CDF for the stress level required to initiate dislocation-mediated flow exhibits an inflection point with each of the examined strain rates. The observed inflection point suggests a peak in the probability density function. For a Weibull distribution, it is then expected that the shape parameter will be near 3. Moreover, the shift of the distribution tail from the origin of the CDF indicates a minimum stress for the

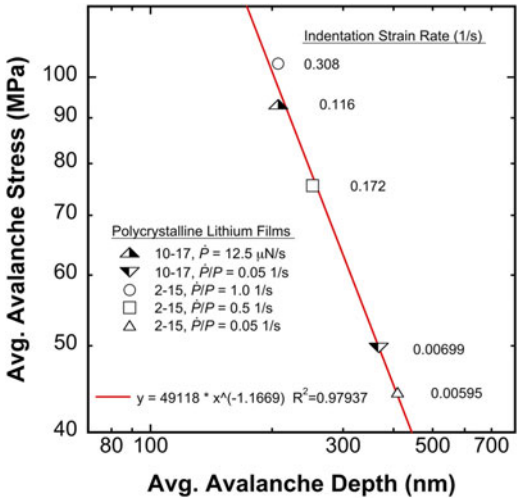

FIG. 2. High-purity vapor deposited Li. Power-law dependence between the average indentation pressure and depth at which the transition from diffusion to dislocation-mediated flow occurs.

initiation of the avalanche, or a nonzero location parameter. A three-parameter Wiebull distribution of the form

$$P = 1 - \exp\left[-\lambda V\left(\frac{\sigma - \sigma_{\text{location}}}{\sigma_{\text{scale}}}\right)^3\right] \quad , \qquad (1)$$

is thus proposed, where P is the cumulative probability, λ is a "critical flaw" number density, and V is the stressed volume. As pointed out by Ngan et al.,[12] Weibull statistics are frequently used in precisely this manner to determine the probability of failure (plastic flow) observed in micropillar and nanoindentation experiments. Of particular interest here, we note that Todinov[13] has demonstrated how the stress terms in a Weibull analysis can be correlated with the length scale of the material defect. Following Todinov's approach as applied to the dislocation source length scale, a physical interpretation of Eq. (1) is possible by hypothesizing that initiation of the transition or avalanche event represents the activation of a Frank–Read source. The mean pressure under the indenter, σ, and the location and scale parameters can then be linked with the dislocation pinning point spacing, L, through

$$\sigma = \frac{Gb}{L} \quad , \qquad (2)$$

$$\sigma_{\text{location}} = \frac{Gb}{L_{\max}} \quad , \qquad (3)$$

and

$$\sigma_{\text{scale}} = \frac{Gb}{L_{\text{ave}}} \quad , \qquad (4)$$

where G is the shear modulus, taken to be 4.25 GPa, b is the magnitude of the Burgers vector, taken to be 3.04 Å, $L_{\max}$ is the maximum spacing for which the entire looping process can occur, and σ_{scale} is the stress that would activate the Frank–Read source having the average length, L_{ave}, in the L distribution (this is not necessarily the average stress). Letting $L_{\max} = \beta h$ and V scale as h^3, where h is the average depth observed for the avalanche, Eq. (1) can now be rewritten as

$$P = 1 - \exp\left[-\lambda {L_{\text{ave}}}^3\left(\frac{Hh}{Gb} - \frac{1}{\beta}\right)^3\right] \quad , \qquad (5)$$

where β is a dimensionless constant that correlates the depth at which the avalanche occurs with the required width of the Frank–Read source capable of completing the entire loop process. Taking values of P near 0.2 and 0.8 for each data set, Eq. (5) was used to solve for β and the product, $\lambda {L_{\text{ave}}}^3$. The values of the calculated terms are shown in Table I and, as shown in Fig. 4, the measured and predicted CDFs compare very well. We, therefore, conclude that Eq. (5) offers one possible rationalization for the mechanism that enables the unique transition from diffusion to dislocation-mediated flow. We also note that evaluation of the proposed CDF at the Weibull mean value, $\bar{H}$, yields

$$\bar{H}h = \frac{Gb\left(\frac{0.885}{L_{\text{ave}}} + \frac{\lambda^{1/3}}{\beta}\right)}{\lambda^{1/3}} \quad , \qquad (6)$$

which directly suggests that the approach is self-consistent in the sense that Eq. (6) predicts the result observed in Fig. 2, where the product $\bar{H}h$ from all five strain rates is nearly a constant, 19.3 N/m ± 6.8%. The experimentally determined values of $\bar{H}h$ are provided in Table I. The implication here is that the avalanche process is correlated with the strain rate through the generation of different diffusion-controlled H–h pathways and that the effect of strain rate on the dislocation source distribution, argued as the Frank–Read source CDF in this paper, has a relatively weak contribution to the observed behavior.

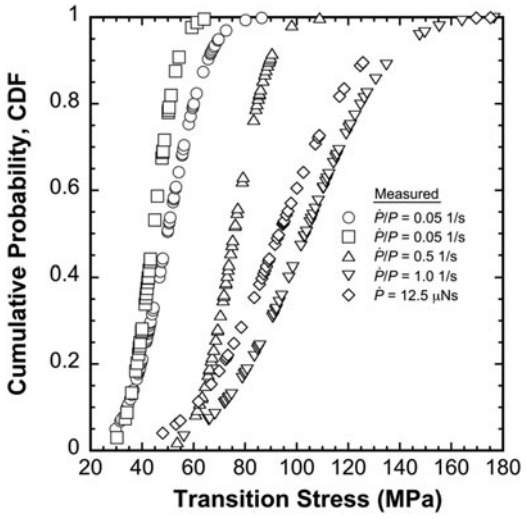

FIG. 3. Experimentally measured CDFs of the indentation pressure (stress) at the sudden transition from diffusion to dislocation-mediated flow.

TABLE I. Values of β and $\lambda {L_{\text{ave}}}^3$ used to calculate the CDF of the transition stress as per Eq. (5) and the experimentally measured Weibull mean value, $\bar{H}h$.

Loading algorithm	β (–)	$\lambda {L_{\text{ave}}}^3$ (–)	$\bar{H}h$ (N/m)
$\dot{P}/P$ = 0.05 s^{-1}	0.200609	9.10666×10^{-4}	18.161
$\dot{P}/P$ = 0.05 s^{-1}	0.129026	2.80198×10^{-3}	18.292
$\dot{P}/P$ = 0.5 s^{-1}	0.108488	4.15534×10^{-3}	19.053
$\dot{P}/P$ = 1.0 s^{-1}	0.173247	5.56022×10^{-4}	21.420
CRL = 12.5 μN/s	0.250707	5.32422×10^{-4}	19.326

B. Displacement burst filter

As previously noted, the magnitude of the displacement burst and the ensuing pressure drop are observed to vary from one test location to the next. We submit not all of the displacement bursts are the result of the proposed Frank–Read mechanism, as some could certainly be caused by traditional or single source dislocation motion. To identify the bursts most likely associated with dislocation multiplication consistent with Frank–Read source looping, a simple metric was used to eliminate measurements that did not meet a minimum plastic strain requirement. Here we use the Orowan equation to express the plastic strain associated with the displacement burst as $\varepsilon_{\text{plastic}} = (h_{\text{burst}}/h_{\text{burst}}^{3})b(2h_{\text{burst}})$. The product $G\varepsilon_{\text{plastic}}$ then corresponds to the pressure drop due to the limited dislocation motion and is taken as the threshold for consideration of dislocation multiplication. Thus, only pressure drops meeting the criteria, $(H_{\text{before burst}} - H_{\text{after burst}}) > 2Gb/h_{\text{burst}}$ are considered. Based on this test-specific metric, 82% of the 325 measurements of h–H burst coordinates performed were found to meet the necessary although not necessarily sufficient criterion for the activation of a Frank–Read source. We note the average values of H_{burst} and h_{burst} with and without the elimination are generally similar, but without the elimination the power law exponent in Fig. 2 decreases by ~11%, from −1.17 to −1.3.

As previously reported, it should be noted that the experimentally estimated pressure drop is overestimated due to the effect of dynamic overload when a displacement burst occurs. The analysis leading to the elimination metric described above is thus inexact. While it is theoretically possible that a displacement-controlled experiment could mitigate or even potentially eliminate dynamic overload, it could only be achieved if the instrument's measurement and control time constants are significantly faster than the time-scale of the displacement burst. At the time of this writing, no known such controller and actuator exist.

C. Grain boundaries act as a dislocation source

Figure 5 is an optical micrograph showing ~220 nm deep residual hardness impressions in one of the largest grains of an 18 μm thick Li film. Under a targeted $\dot{P}/P$ of 0.05 s^{-1}, the grain interior and boundary were sampled 28 and 68 times, respectively. As the image shows, the test sites are generally within 1–3 μm of the grain boundary and the orientation of the tip relative to the boundary changes from one test site to the next. Figure 6 directly compares CDFs of the avalanche stress as measured in the grain interior and near the boundary. Although estimating the magnitudes and physical dimensions of the elastic stress field under load is difficult due to the diffusional creep, the CDFs shown in Fig. 6 clearly indicate that the boundary acts as a dislocation source at 31 °C, as indents positioned near the boundary require less stress to initiate the transition to dislocation-mediated flow. As explained by Hirth and Lothe,[14] a variety of grain boundary sources exist. Among the possibilities are stress concentrations at the boundary that preferentially operate nucleation sources or small angle nets acting as Frank–Read sources. We further note that this observation is generally consistent with nanoindentation studies and atomistic simulations performed on gold films.[15]

D. Implications of lithium's mechanical behavior at small length scales in relation to potential failure mechanisms of SEs

The unique mechanical behavior of Li at small length scales and high T_{H} is of particular interest because of its

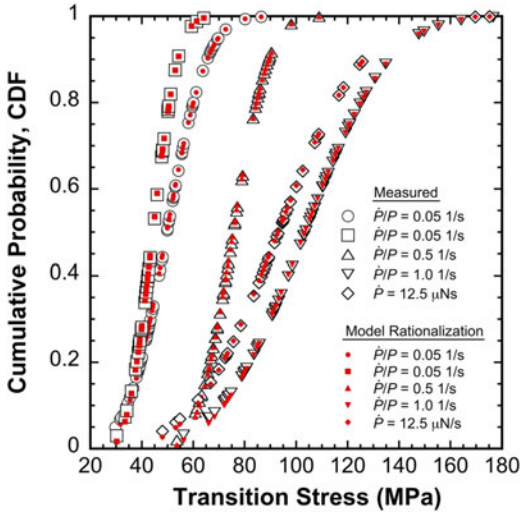

FIG. 4. CDFs of the indentation pressure (stress) at the sudden transition from diffusion to dislocation-mediated flow: Direct comparisons between the experimentally measured CDFs and rationalizations based on the activation of a Frank–Reed source at the transition stress.

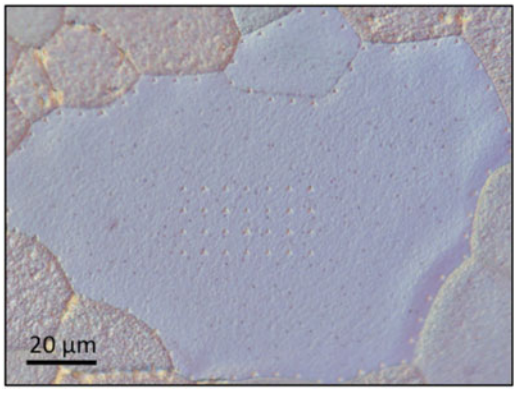

FIG. 5. Optical micrograph of ~220 nm deep indents in a high-purity vapor deposited 18 μm thick Li film on a glass substrate: 28 indents in the interior of the grain and 68 indents in close proximity to the grain boundary.

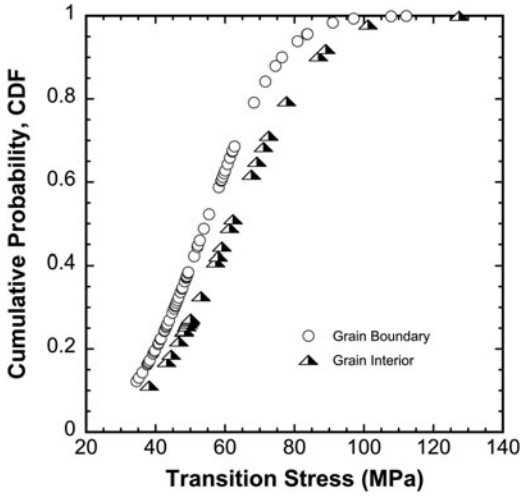

FIG. 6. Direct comparison between the experimentally measured CDFs of the indentation pressure (stress) at the sudden transition from diffusion to dislocation-mediated flow in the grain interior versus close proximity to the grain boundary. This result clearly indicates that the grain boundary acts as a dislocation source.

potential impact on the performance of energy storage devices. During charging, gradients in the chemical potential will force Li to preferentially diffuse into defects at the Li/SE interface. In a manner that depends on the length scale of the interfacial defect and the imposed strain rate, the reported results show at a T_H of 0.67 and an initially low dislocation density ($\rho \leq 1.1 \times 10^{12}$ m^{-2}), Li can support pressures ranging from ~46 to 350 times higher than the nominal yield strength of bulk polycrystalline Li.[3] The highest pressures developing in the smallest interfacial defects exposed to the highest strain rates. Here we propose the strain rate is directly coupled to the charging current density.

Grain boundaries, grain boundary grooving, porosity, and scratches in the SE separator are among the potential small-scale defects disrupting the local Li/SE interface morphology. During charging, these defects would become filled with metallic Li at a rate that depends on the current density. Here we assume the constraint afforded by the high elastic modulus of the SE separator inhibits volume expansion of the Li inside the defect and results in a hydrostatic pressure component analogous to that of a rigid, thick-walled pressure vessel, with hoop stresses developing at the Li/SE interface. The difference from the pressure vessel analogy is that the hydrostatically stressed Li is open to the planar Li film outside the defect, allowing for the possibility of stress relief by diffusion or dislocation-mediated flow.

For an interfacial defect in the physical form of a groove with a radius, R, and a fixed length, L, the time dependence of the volumetric strain due to an increase in R caused by the influx of Li may be written in terms of the current density (to a first order approximation) as

$$\frac{\mathrm{d}}{\mathrm{d}t}\frac{\Delta V}{V} = \frac{2}{R}\frac{\mathrm{d}R}{\mathrm{d}t} = \frac{2}{R}\frac{iA\Omega}{F} \quad , \tag{7}$$

where i is the charging current density ($i < 0$), A is Avogadro's number, Ω is the atomic volume of Li, and F is the Faraday constant. In the absence of any plasticity, the radial elastic strain rate due to the incorporation of Li within the groove is

$$\dot{\varepsilon}_{\mathrm{elastic}} = \frac{2}{R}\frac{\mathrm{d}R}{\mathrm{d}t} = \frac{2}{R}\frac{iA\Omega}{F} \quad . \tag{8}$$

Using the previously adopted conservation of strain approach,[3] $|\dot{\varepsilon}_{\mathrm{elastic}}| = |\dot{\varepsilon}_{\mathrm{total}}| - |\dot{\varepsilon}_{\mathrm{plastic}}|$, it naturally follows that if plasticity contributes to the change in R, then

$$|\dot{\varepsilon}_{\mathrm{elastic}}| = \left|\frac{2}{R}\frac{iA\Omega}{F}\right| - |\dot{\varepsilon}_{\mathrm{plastic}}| \quad . \tag{9}$$

In the case of a kinetically limited plasticity mechanism for relief of the hydrostatic pressure, p, the time dependence of the hydrostatic pressure due to charging is then

$$\left|\frac{\mathrm{d}p}{\mathrm{d}t}\right| = K\left[\left|\frac{2}{R}\frac{iA\Omega}{F}\right| - |\dot{\varepsilon}_{\mathrm{plastic}}|\right] \quad , \tag{10}$$

where K is the bulk modulus. A simple Thevenin equivalent circuit model for charging ($i < 0$) applied locally at the groove is proposed for extending the analysis to consider the relationship between stress relief mechanisms and the electrochemical parameters in the most transparent manner. The charging voltage is correlated with the current density at the groove through

$$V_{\mathrm{applied}} = \mathrm{OCV} - \frac{i(2\pi RL)R_{\mathrm{BattA}}}{2\pi RL} \quad , \tag{11}$$

where R_{BattA} is the area specific battery internal resistance (Ohm m^2 = (J s)/C^2 m^2) and OCV is the open circuit voltage. The OCV is a function of the hydrostatic stress at the groove ($P < 0$), given by

$$\mathrm{OCV} = \mathrm{OCV_o} - \frac{\Omega p A}{F} \quad , \tag{12}$$

where $\mathrm{OCV_o}$ is the stress free open circuit voltage.[16] The current density at the groove can then be determined by combining Eqs. (11) and (12) as

$$|i| = \frac{V_{\mathrm{applied}} - \mathrm{OCV_o} - \frac{A\Omega|p|}{F}}{R_{\mathrm{BattA}}} \quad , \tag{13}$$

where for small defects ($R \leq$ ~500 nm based on the results reported here and a previous publication),[3] the

length scale may not allow glide-controlled dislocation mechanisms such as Frank–Reed sources to operate at stresses near the bulk yield strength. Under these conditions, dislocation plasticity will not be an efficient stress relief mechanism, allowing the hoop stress within the interfacial defect to build to values capable of initiating mode I fracture in the SE. In the absence of dislocation mediated plasticity, at very large gradients in stress (for small R), alternative stress relief mechanisms in Li may operate, particularly diffusional processes due to the large homologous temperature. A diffusional creep mechanism would be expected to operate at small R, as the gradient in chemical potential due to the hydrostatic stress gradient is proportional to $1/R$. By analogy with Nabarro–Herring creep rate kinetics, the plastic strain rate term in Eq. (10) is expected to have the form

$$\left|\dot{\varepsilon}_{\text{plastic}}\right| = \left|\frac{D\Omega}{k_{\text{B}}T}\frac{p}{R^2}\right| \quad . \tag{14}$$

Substituting Eqs. (13) and (14) into Eq. (10) yields a steady state ($\mathrm{d}p/\mathrm{d}t = 0$) hydrostatic stress magnitude given by

$$|p| = \frac{2AF\left(V_{\text{applied}} - \text{OCV}_{\text{o}}\right)}{2A^2\Omega + \left(DR_{\text{BattA}}\right)\frac{F^2}{Rk_{\text{B}}T}} \quad . \tag{15}$$

It is noted with some satisfaction that the kinetic terms, D and R_{BattA}, are lumped together such that at $D = 0$, only the thermodynamic terms will determine p. It may also be seen that the geometric dependence (on R) is removed at $D = 0$. However, as the diffusion coefficient increases, the magnitude of p decreases and the positive correlation between the magnitude of p and R (proportional to the diffusion length) is emphasized. Due to the large thickness of the SE relative to the dimensions of the interfacial defect, the hoop stress acting at the Li/SE interface will be approximately equal in magnitude to p. We note the analogy of Eq. (15) with the nanoindentation results is that the high indentation strain rates correlate with a high current density and the length scale of the indentation corresponds to the length scale of the defect at the Li/SE interface. Based on the indentation results and the analysis here for high charging current densities, the high stresses at the Li/SE interface are expected when the length scale is large enough to inhibit diffusional relaxation, but not large enough to allow for the initiation of mobile glide dislocation multiplication.

IV. CONCLUSIONS

(1) Based on a total of 325 measurements performed at 31 °C and targeted $\dot{P}/P$ values of 0.05, 0.5, and 1.0 s^{-1} and a constant $\dot{P}$ of 12.5 μN/s, the transition from diffusion to dislocation-mediated flow in vapor deposited Li films is found to occur at average mean pressures of approximately 44, 75, 104, and 93 MPa, respectively. Assuming a constraint factor of 1, these stresses range from roughly 88 to 208 times higher than the nominal yield strength of polycrystalline Li near room temperature. These observations are generally consistent with the microcompression experiments recently performed by Xu et al.,[1] who observed that the compressive yield strength of single crystal Li increases from 15 to 105 MPa as the pillar diameter decreases from 9.45 to 1.39 μm (approximately 30–210 times larger than the yield stress of bulk polycrystalline Li).

(2) A subset of 268 measurements encompassing 4 loading algorithms spanning indentation strain rates from 0.00595 to 0.308 s^{-1} show a significant size effect in the transition stress versus depth with a power law exponent of −1.17. This size effect is controlled by the size of the indentation stress field in relation to the defect structure being sampled by the indenter rather than the physical dimensions of the test specimen. The exponent obtained here is almost double the value obtained from Xu's[1] microcompression experiments (−0.68) at a slightly lower T_{H}.

(3) At 31 °C, grain boundaries in Li act as dislocation sources, as the stress level required to initiate the transition to dislocation-mediated flow is discernibly less in close proximity to a boundary.

(4) A mechanistic rationalization of the transition to dislocation-mediated flow is provided by the activation of a Frank–Read source. Excellent agreement is found between the experimental CDF and the CDF hypothesized for activation of the Frank–Read source. The important implication is that the local defect structure and diffusion-controlled H–h pathways determine the stress at the transition.

(5) In the limit of diffusion rather than dislocation-mediated flow, a Thevenin equivalent circuit has been used to predict the hydrostatic pressure in a defect at the Li/SE interface based on the charging current density and the electrochemical parameters of the cell, Eq. (15).

(6) Rationalization of the depth and strain-rate dependent hardness of lithium presented here and in the previous work suggests that under certain conditions, a brittle SE separator may be susceptible to failure by mode I fracture initiating at small-scale defects at the Li/SE interface. The conditions most conducive to fracture are as follows: (i) a moderate or low initial dislocation density in the lithium ($\leq\sim 9.4 \times 10^{11}$ m^{-2}); (ii) a high homologous temperature ($\geq$0.67); (iii) defects physically too small ($\leq\sim$500 nm) to activate glide-controlled dislocation sources; and (iv) high charging current densities.

ACKNOWLEDGMENTS

This research was sponsored jointly by the U.S. Department of Energy, Office of Energy Efficiency and Renewable Energy's Advanced Battery Materials Research program (managed by Tien Duong) and by TARDEC, the U.S. Army Tank Automotive Research Development and Engineering Center. E.G.H. is grateful for start-up funding from the Department of Materials Science and Engineering at Michigan Technological University. V.T.'s contributions were financially supported through the MSE department's McArthur Internship program.

REFERENCES

1. C. Xu, Z. Ahmad, A. Aryanfar, V. Viswanathan, and J.R. Greer: Enhanced strength and temperature dependence of mechanical properties of Li at small scales and its implications for Li metal anodes. *Proc. Natl. Acad. Sci. U.S.A.* **114**, 57 (2017).
2. R. Schultz: *Lithium: Measurement of Young's Modulus and Yield Strength*; Technical Report FERMILAB-TM-2191; Fermi National Accelerator Laboratory: Batavia, IL, 2002.
3. E.G. Herbert, S.A. Hackney, N.J. Dudney, V. Thole, and P.S. Phani: Nanoindentation of high purity vapor deposited lithium films: A mechanistic rationalization of diffusion-mediated flow. *J. Mater. Res.* **33**, 1347–1360 (2018).
4. P.S. Phani, K.E. Johanns, E.P. George, and G.M. Pharr: A stochastic model for the size dependence of spherical indentation pop-in. *J. Mater. Res.* **28**, 2728 (2013).
5. O. Kraft, P.A. Gruber, R. Mönig, and D. Weygand: Plasticity in confined dimensions. *Annu. Rev. Mater. Res.* **40**, 293 (2010).
6. M. Stricker and D. Weygand: Dislocation multiplication mechanisms—Glissile junctions and their role on the plastic deformation at the microscale. *Acta Mater.* **99**, 130 (2015).
7. J.A. El-Awady: Unravelling the physics of size-dependent dislocation-mediated plasticity. *Nat. Commun.* **6**, 5926 (2015).
8. Y. Li, A.J. Bushby, and D.J. Dunstan: The Hall–Petch effect as a manifestation of the general size effect. *Proc. R. Soc. London, Ser. A* **472**, 20150890 (2016).
9. E.G. Herbert, S.A. Hackney, N.J. Dudney, and P.S. Phani: Nanoindentation of high purity vapor deposited lithium films: The elastic modulus. *J. Mater. Res.* **33**, 1335–1346 (2018).
10. G. Feng and A.H.W. Ngan: Creep and strain burst in indium and aluminium during nanoindentation. *Scr. Mater.* **45**, 971 (2001).
11. L. Bragg: A theory of the strength of metals. *Nature* **149**, 511–513 (1942).
12. A.H.W. Ngan, L. Zuo, and P.C. Wo: Size dependence and stochastic nature of yield strength of micron-sized crystals: A case study on Ni_3Al. *Proc. R. Soc. London, Ser. A* **462**, 1661 (2006).
13. M. Todinov: Is Weibull distribution the correct model for predicting probability of failure initiated by non-interacting flaws? *Int. J. Solid Struct.* **46**, 887 (2009).
14. J.P. Hirth: The influence of grain boundaries on mechanical properties. *Metall. Trans.* **3**, 3047 (1972).
15. E. Lilleodden and W.D. Nix: Microstructural length-scale effects in the nanoindentation behavior of thin gold films. *Acta Mater.* **54**, 1583 (2006).
16. J.W. Gibbs: On the equilibrium of heterogeneous substances. In *The Scientific Papers of J. Willard Gibbs*, Vol. **1** (Longmans, Green, London, U.K., 1906); pp. 55–349.